Spin-polarized 2D ACAR in nickel across the Curie temperature

1991 J. Phys.: Condens. Matter 3 4201

(http://iopscience.iop.org/0953-8984/3/23/009)

J. Phys.: Condens. Matter 3 (1991) 4201–4212. Printed in the UK

Spin-polarized 2D ACAR in nickel across the Curie temperature

P Genoud, A A Manuel, E Walker and M Peter
Département de Physique de la Matière Condensée, Université de Genève,
24 Quai Ernest Ansermet, CH-1211 Genève 4, Switzerland

Received 28 December 1990, in final form 8 March 1991

Abstract. We present two-dimensional angular correlation of (polarized positrons) annihilation radiation (2D ACAR) results measured on a single crystal of Ni in the (100) plane below and above the Curie temperature (at 4.2, 300, 600 and 660 K). The experimental distributions (total momentum density) measured at different temperatures do not exhibit any significant differences, in contradiction to the one-dimensional (non-spin-polarized) results of Kontrym-Sznajd *et al*. We conclude that the Fermi surface topology of Ni essentially does not change between 4.2 and 600 K. This can be related to the fact that the exchange splitting, Δ, remains almost constant up to the Curie temperature. This would confirm the spin-polarized electron-energy-loss spectroscopy results of Kirschner and Langenbach.

1. Introduction

The study of the angular correlation of (positron) annihilation radiation (ACAR) has been, at a very early stage, exploited to investigate the momentum distribution of the electrons responsible for ferromagnetism. Pioneers in this field were Hanna and Preston (1958) who succeeded in experimentally showing the negative polarization of the s and p conduction electrons of ferromagnetic iron. Many ACAR results followed, which were mainly concerned with ferromagnetic transition metals as well as with rare earths (see the reviews by Berko 1977 and Mijnarends 1979). Surprisingly, despite its potential efficiency, the two-dimensional ACAR (2D ACAR) technique has not been applied to the investigation of the spin-density in momentum space so often: we have only quoted the works of Hoffmann *et al* (1982) in Gd, Jarlborg *et al* (1986) in Ni and Genoud *et al* (1988) in Fe. On the other hand, the Compton profile experiments are growing in number due to improvements in technique, and spin-density in momentum space has already been measured in Ni by Mills (1987). Experimental 'positron undisturbed' $\rho(p)$ data are thus available, but only with a low resolution and integrated over two momentum components. Moreover, the relatively small value of the magnetic moment of Ni (when compared with Fe or Co) leads to poor statistical accuracy.

Two factors have motivated the present study: first, a two-dimensional measurement of the spin-density in momentum space as a function of temperature has never been done before. Such a measurement highlights the possibilities offered by the 2D ACAR technique in the study of magnetic materials even if the interpretation of the results is complicated by the presence of the positron wave function and of the 3γ processes. Our

0953-8984/91/234201 + 12 $03.50

second interest was to answer the question of whether or not the Fermi surface (FS) topology of Ni is modified when going through the Curie temperature (T_{Curie}(Ni) = 627 K) as stated by Kontrym-Sznadj *et al* (1975) after analysis of 1D ACAR data and indirectly by Yousuf *et al* (1986) on the basis of high-temperature electrical resistivity measurements. These latter results are in contradiction with angle-resolved photoelectron spectroscopy (Hopster *et al* 1983, Gerhard 1983) and with spin-polarized electron-energy-loss spectroscopy measurements (Kirschner and Langenbach 1988) which exhibit a non-vanishing exchange splitting, Δ, above T_{Curie}, such a behaviour being incompatible with an important change of the FS topology. As the 2D ACAR technique is not drastically limited by high temperatures in the study of FS, we have measured, at 4.2, 300, 600 and 660 K, the total and spin momentum densities of a single crystal of Ni. The answer to whether or not the FS of Ni changes on crossing T_{Curie} can then be directly related to the behaviour of Δ across the magnetic transition.

The outline of the present paper is as follows. Section 2 gives a brief theoretical summary of a spin-polarized 2D ACAR measurement in a ferromagnetic crystal. In section 3 we present the experimental details and the data analysis procedure. Section 4 contains a discussion of the results, and in section 5 we state our conclusions.

2. Positron annihilation in a ferromagnetic material

In a magnetized ferromagnetic crystal the number and the distribution of electrons are different for those with their spin parallel or antiparallel to the magnetization. As already discussed in detail by Berko and Zuckermann (1964) and by Berko and Mills (1971), the ACAR technique allows one to measure this difference, using polarized positrons. In effect, due to parity non-conversation in β-decay, most of the positrons are emitted from a source with their spin pointing in the forward direction and this is independent of the direction of the magnetic field applied to saturate the sample. Thus reversing the magnetic field direction will reverse the polarization of the electronic spins but not that of the positron beam. As the thermalization process only slightly reduces the polarization of the positrons (Page 1959, Blank *et al* 1988), it is possible to investigate the spin density of ferromagnetic materials. This is due to the annihilation selection rules which state that a polarized positron and a spin-aligned electron anihilate from a singlet state (2γ annihilation) or, with a much smaller probability, from a triplet state (3γ annihilation), depending on whether the spin of the electron is antiparallel or parallel to the spin of the positron.

A typical experiment consists, then, in measuring the 2D ACAR surfaces $N\uparrow(p_x, p_y)$ and $N\downarrow(p_x, p_y)$ with the magnetic field respectively parallel and antiparallel to the positron majority spins. Each measured 2D ACAR distribution can be expressed as:

$$N\uparrow(\downarrow)(p_x, p_y) = \int [A^{\uparrow(\downarrow)}\rho^{2\gamma}_{maj}(\boldsymbol{p}) + (1 - A^{\uparrow(\downarrow)})\rho^{2\gamma}_{min}(\boldsymbol{p})]\, dp_z \qquad (1)$$

where $\rho^{2\gamma}_{maj}(\boldsymbol{p})$ and $\rho^{2\gamma}_{min}(\boldsymbol{p})$ are the momentum densities seen by positrons for both electronic spin directions. $A^{\uparrow(\downarrow)}$ is a constant depending on the magnetic field direction, the positron spin polarization P_p and the so-called $P_{3\gamma}$ factor, which describes the 3γ corrections but is difficult to measure precisely. As discussed by Berko and Mills (1971), the existence of these 3γ processes complicates the interpretation of the experimental distributions (with both magnetic field directions) directly in terms of total and spin momentum densities. To compare the measurements obtained at different temperatures

we prefer to follow the method proposed by Rabou (1983), who adds or subtracts the experimental 2D ACARS $N\uparrow(\downarrow)(p_x, p_y)$ after normalization to the unit volume:

$$\Sigma N(p_x, p_y) = N\uparrow(p_x, p_y)/N\uparrow + N\downarrow(p_x, p_y)/N\downarrow \tag{2}$$

$$\Delta N(p_x, p_y) = N\uparrow(p_x, p_y)/N\uparrow - N\downarrow(p_x, p_y)/N\downarrow \tag{3}$$

where $N\uparrow$ and $N\downarrow$ are the volumes of the corresponding 2D ACAR spectra. Then the resulting distributions can be directly interpreted as relative total momentum density $\Sigma N(p_x, p_y)$ and relative spin momentum density $\Delta N(p_x, p_y)$:

$$\Sigma N(p_x, p_y) = \rho^{2\gamma}_{\min}(p_x, p_y)/\rho^{2\gamma}_{\min} + \rho^{2d}_{\mathrm{maj}}(p_x, p_y)/\rho^{2\gamma}_{\mathrm{maj}} \tag{4}$$

$$\begin{aligned}\Delta N(p_x, p_y) &= -P_p[\rho^{2\gamma}_{\min}(p_x, p_y)/\rho^{2\gamma}_{\min} - \rho^{2\gamma}_{\mathrm{maj}}(p_x, p_y)/\rho^{2\gamma}_{\mathrm{maj}}] \\ &= -\mathrm{const}[(\rho^{2\gamma}_{\mathrm{maj}}/\rho^{2\gamma}_{\min})\rho^{2\gamma}_{\min}(p_x, p_y) - \rho^{2\gamma}_{\mathrm{maj}}(p_x, p_y)]\end{aligned} \tag{5}$$

where $\rho^{2\gamma}_{\mathrm{maj}}(p_x, p_y)$ and $\rho^{2\gamma}_{\min}(p_x, p_y)$ represent the momentum densities of either spin direction and as seen by the positron, integrated over the p_z component; $\rho^{2\gamma}_{\min}$ and $\rho^{2\gamma}_{\mathrm{maj}}$ are the volumes of the corresponding distributions.

3. Experimental details and data analysis

The 2D ACAR surfaces $N\uparrow(\downarrow)(p_x, p_y)$ in the (100) plane of a single crystal of nickel were measured at 4.2, 300, 600 and 660 K with a resolution of (0.5×0.8) mrad^2 at 4.2 K. We chose 0.20 mrad/bin as the mesh of the histogram, covering a momentum of ± 40 mrad in both x and y directions. Our γ-ray detectors consist of two high-density proportional chambers (Bisson *et al* 1982) with an increased sensitive area of 30×30 cm^2. The detector–sample distance has been set to 4.98 m. Measurements were performed under vacuum ($<10^{-5}$ Torr), in a partially polarized positron beam emitted by a 50 m Ci^{22}Na source for both up and down magnetic field directions (parallel to the [011] direction). The magnetic field intensity was set to 4 T in order to saturate the sample and to focus positrons on it. A copper sample holder has been mounted on a resistive coil designed to heat the sample up to more than 660 K. The temperature (stabilized to ± 1 K) was measured with a platinum resistor. The single crystal of nickel was obtained by zone melting and further annealed for 12 h at 1000 °C. Lifetime measurements (using a standard fast–fast spectrometer as described by Badwell and Paulus 1979) indicate essentially a single component at 108 ± 2 ps. This suggests that almost no trapped positrons contributed to the measurements.

The 2D ACAR distributions $N\uparrow(\downarrow)(p_x, p_y)$ have been measured for a crystal orientation with the integration axis p_z along the [100] direction by collecting about 3×10^8 total counts for each magntic field direction ($\uparrow$, $\downarrow$). The total 2D ACAR (the spin density spectrum) is obtained by adding (subtracting) these two distributions after normalization to the unit volume. The very high statistics are necessary to extract a spin density signal with an acceptable precision.

The raw measured 2D ACAR histograms were corrected with the experimental angular efficiency distribution, evaluated in each case on a set of 10^9 events. We did not smooth the total momentum distributions. This allows us to consider every experimental point as independent when comparing the spectra and excludes any artefact that could be due to the smoothing procedure. Anyway, the statistics are sufficiently good and the error

bars remain small enough when compared with the FS related structures. The spin density in Ni corresponds, however, to a very weak signal and in order to reduce the statistical noise we have smoothed these distributions by convoluting them with a square function of (1.6×1.6) mrad^2. Following the method proposed by Rabou (1983), we present in this work only relative distributions $\Delta N(p_x, p_y)$ and $\Sigma N(p_x, p_y)$ as defined in (2) and (3).

In order to exhibit the anisotropies of the total 2D ACAR distributions, we have subtracted the part that is invariant to rotations; this isotropic part is calculated for a set of equidistant p radii as the mean value of the 2D ACAR and has been smoothed before subtraction. This confirmed the correct orientation of our sample allowing us, then, to fold the distributions along the symmetry lines of the investigated (100) plane. The analysis has been undertaken on these folded distributions.

The LCW theorem (Lock *et al* 1973) on the remapping of the ACAR from p to k space has been applied to the total 2D ACARs measured at different temperatures in order to investigate a possible modification of the FS topology when going through T_{Curie}. This analysis has been performed following the procedure:

$$F(k_x, k_y) = \sum_{G_x, G_y} N(k_x + G_x, k_y + G_y) \tag{6}$$

where G_x and G_y are the components of the reciprocal vectors in the (p_x, p_y) plane. The temperature dependence of the lattice constant a has been taken into account in the analysis ($a(T) = 3.5166 + 3.227 \times 10^{-5} \times T[\text{K}])$ Å).

As shown by the *ab initio* calculations of Jarlborg and Singh (1987) and of Sormann (1988), the positron wave function together with the electron–positron correlation effects play a rather important role in ferromagnetic Ni, preventing an analysis of the LCW distributions directly in terms of a projection of the FS on the investigated (100) plane. A modified FS topology should, however, be reflected in these distributions.

4. Results and discussion

4.1. Total momentum density

The analysis of the total 2D ACAR distributions $\Sigma N(p_x, p_y)$ measured at different temperatures has been mainly performed in k space since this is the natural way of proceeding when dealing with FS related structures. However, to confirm the conclusions obtained in k space, we have also compared the distributions directly in p space as described below. For a complete presentation of the experimental data, we show in figure 1 the contour plot of the anisotropic part of the 2D ACAR spectrum measured at 4.2 K in the (100) plane of our Ni single crystal. The data obtained at 300, 600 and 660 K look very similar; we only notice a reduction of the amplitude of the anisotropy with increasing temperature. When compared with the maximum amplitude of the corresponding total 2D ACARs we obtain the values of 6.08, 5.47, 4.94 and 4.64% for the measurements at 4.2, 300, 600 and 660 K, respectively. This certainly reflects the reduction of the experimental resolution with the temperature increase.

To answer the question of whether the FS of Ni would change through the magnetic transition we have first considered the LCW-folded distributions measured at different temperatures. Kontrym-Sznajd *et al* (1975) predict a FS for paramagnetic Ni similar to that of Pd, with, however, a fifth sheet which should be smaller and a sixth one which

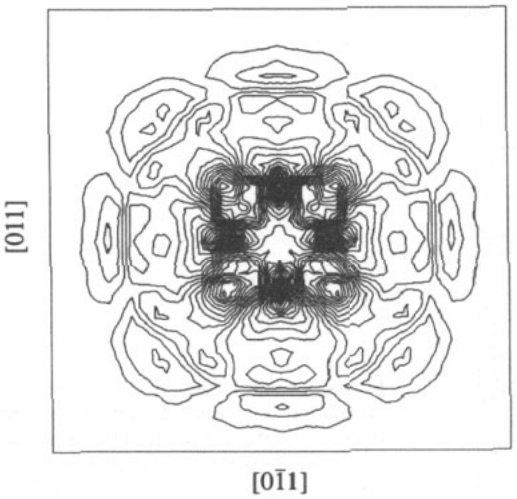

Figure 1. Contour plot of the anisotropic part of the total 2D ACAR of Ni measured in the (100) plane at 4.2 K. The levels are spaced by 3% of the total amplitude of the anisotropy. We have only represented an area of ± 20 mrad in both x and y directions. The distribution has been folded for presentation.

should be larger. With regard to the ferromagnetic phase the occupied majority spin states of the fifth sheet would then be empty for momenta close to the Brillouin zone boundary. These authors, comparing reconstructed $\rho^{2\gamma}(\boldsymbol{p})$ distributions, claim to have observed such a regrouping. They also noted a sixth sheet of the FS that is more spherical in the paramagnetic than in the ferromagnetic state and also shows a modification of the shape of the [111] necks (from conical to cylindrical). Such changes in the electronic band structure of Ni have been indirectly confirmed by Yousuf *et al* (1986) who have measured the electrical resistivity of Ni under pressure on crossing the magnetic transition. These authors qualitatively explain the observed anomalous behaviour of the resistivity near T_{Curie} by assuming that the band structure changes at this temperature.

The modifications of the FS topology of Ni when undergoing the magnetic transition as described by Kontrym-Sznajd *et al* (1975) should be unambiguously identified with a 2D ACAR experiment if we consider that the structures of the LCW distributions that we have measured in the (100) plane are very large: they represent more than 20% of the total amplitude of the LCW-folded spectrum. A drastic redistribution of the electrons above T_{Curie} would then produce a signature far above the statistical noise. However we have to consider the influence of the intense saturating magnetic field set on the sample. As shown below, it induces a magnetization above T_{Curie} whose effects on the electronic occupancy probability are unknown. The data measured by Kontrym-Sznajd *et al* do not suffer from this problem. Effectively these 1D ACAR distributions have been obtained without applying any magnetic field to the sample. On the other hand, as the positron beam is polarized, a zero-field measurement can lead to different results, depending on whether the sample has been previously magnetized or not. Thus an ACAR experiment under zero magnetic field requires careful attention to the magnetization state of the sample below T_{Curie}. From this point of view, the saturating magnetic filed guarantees an unambiguous measurement of $\Sigma N(p_x, p_y)$ and $\Delta N(p_x, p_y)$.

We have compared the LCW-folded distributions measured at 4.2, 300, 600 and 660 K taking into account a temperature-dependent lattice constant as described in section 3. We present in figure 2 the contour plot of the LCW-surface corresponding to the 4.2 K measurement. We do not observe drastic changes at higher temperatures as shown in figure 3 where lines along high symmetry directions are extracted from each LCW

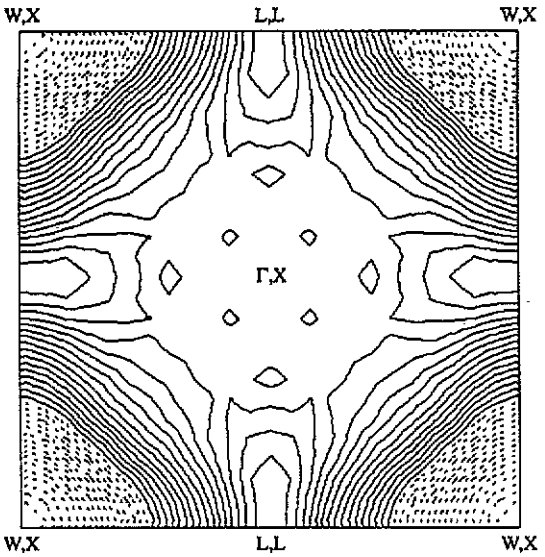

Figure 2. Contour plot of the LCW surface of Ni (total momentum density) measured in the (100) plane at 4.2 K. The levels are spaced by 3% of the total amplitude of the non-constant part of the distribution. The full curves represent the upper levels.

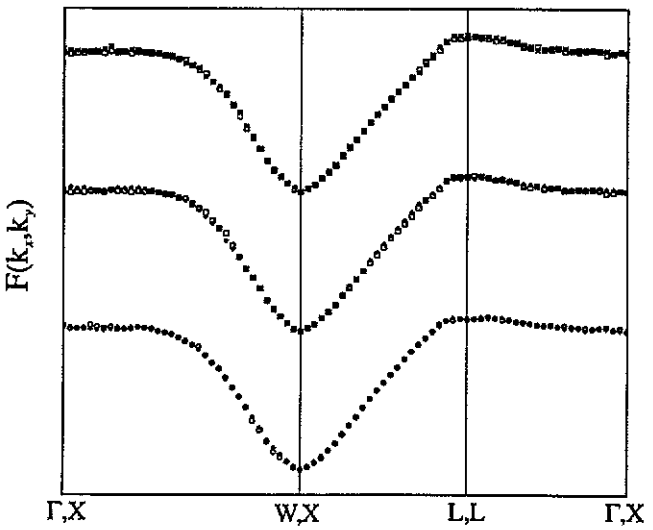

Figure 3. LCW distributions $F(k_x, k_y)$ of Ni (total momentum density) Measured at different temperatures represented along some high symmetry lines of the Brillouin zone. Only the non-constant part of the spectrum is drawn after normalization to unit volume. *: 4.2 K, □: 300 K, ◆: 600 K, ○: 660 K. The size of statistical error bars is the same as that of the symbols. Each point represented is statistically independent.

distribution. The non-constant part of the spectrum is normalized to unit volume before comparison. When considering the statistical error bars and the importance of the FS-related signals in Ni (Singh *et al* 1986), we can conclude that these four distributions essentially reflect the same FS topology. To complete our analysis we have also calculated the derivative of a $p_y = 0$ line extracted from the 2D ACARS measured between 4.2 and

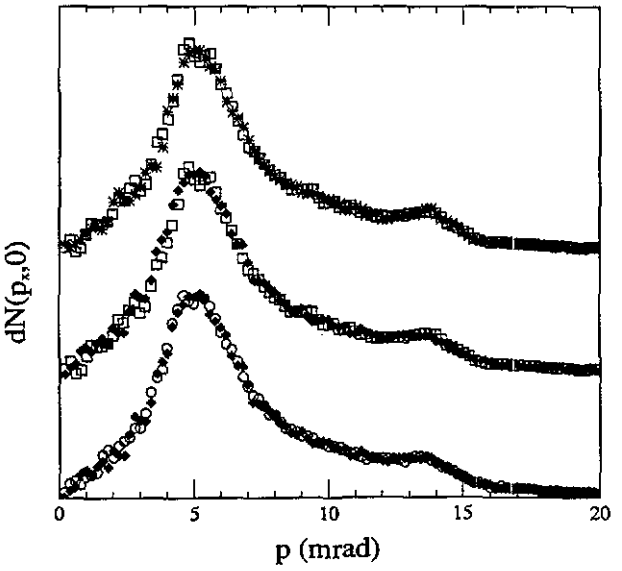

Figure 4. Derivatives of the [110] line extracted from the total 2D ACARs measured in the (100) plane of Ni at 4.2 K (*), at 300 K (□), at 600 K (◆) and at 660 K (○). The two distributions have been normalized to the same volume for comparison. Each point represented is statistically independent. In the low-momentum region ($p_x < 10$ mrad) the size of the error bars is approximately one and half that of the symbols.

660 K. For each experimental point $N(p_x, 0)$ on this line, the derivative (in arbitrary units) is taken as $N(p_x + \Delta p_x, 0) - N(p_x - \Delta p_x, 0)$ where Δp_x is the mesh of the histograms. The corresponding curves presented in figure 4 do not show any difference larger than the statistical noise. Thus both analyses (in $\boldsymbol{p}$ and $\boldsymbol{k}$ space) lead to the same conclusion, that changes in the FS of Ni are not observed between 4.2 and 660 K (under a magnetic field of 4 T).

The absence of any significant difference between the LCW distributions measured at 4.2, 300 and 600 K can be interpreted as the manifestation of an exchange splitting Δ, quasi-independent of the temperature. In order to estimate the maximum variation of Δ that would be consistent with our experimental data we have calculated, following the method proposed by Singh and Jarlborg (1985), the 2D ACAR of ferromagnetic Ni in the (100) plane using LMTO (linear muffin-tin orbitals) wave functions. Electron–positron correlation effects of Jarlborg and Singh (1987) are included through a density dependent enhancement factor in which both electrons and positrons are considered to be free from lattice interaction ($m^* = \frac{1}{2}$). The resulting LCW distribution agrees relatively well with the experiment (Jarlborg and Singh 1987) in spite of unsolved problems common to every self-consistent band-structure calculation (over large exchange splitting and magnetic moment, imperfect FS topology). The reduction of the exchange splitting (originally of about 47 mRyd) was simulated by a rigid band shift, in opposite directions for the majority (down-shift) and for the minority (up-shift) electrons and with the constraint of charge conservation. The calculated distributions, convoluted with the experimental resolution, reveal that a reduction of Δ down to 34 mRyd could possibly not be detected when comparing our experimental 2D ACAR data. Below this value we should, however, clearly observe the differences induced in the distributions by a further

reduction of Δ. Thus we cannot exclude a reduction of the exchange splitting of about 28% between 4.2 and 600 K. But this remains a crude approximation, due to the diffiulties encountered in the self-consistent band calculations in describing the electronic structure of ferromagnetic Ni (see above) and to the fact that we have simulated a reduction of Δ with a rigid band shift which perhaps badly describes the situation. Thus our analysis is not detailed enough to decide unambiguously whether the exchange splitting decreases slightly with increasing temperature or whether it remains eseentially independent of temperature up to T_{Curie} as proposed by Kirschner and Langenbach (1988) after their study of spin-polarized electron-energy-loss spectroscopy data. But the structures of the LCW distributions measured at different temperatures change so little (see figure 3) that we would exclude the important variation of Δ proposed by Hopster *et al* (1983) and by Gerhard (1983) on the basis of angle-resolved photoelectron spectroscopy. Our interpretation naturally contradicts the results of the Stoner model which predicts a zero value of Δ at T_{Curie}, leading to a paramagnetic band structure.

The observation that the LCW distribution measured at 660 K does not exhibit any significant difference from that measured at 600 K is not that helpful because our measurements have been carried out under an intense magnetic field of 4 T. This does not modify the above conclusions concerning the FS topology but we have to keep in mind that the data obtained at 660 K still correspond to a measurement in a magnetized state (see section 4.2). We can then only conclude that above T_{Curie} and under an intense magnetic field the exchange splitting remains basically constant. We have, however, no information about the paramagnetic state (zero-field measurement) for which high statistics 2D ACAR data would be desirable.

4.2. Spin density

The very high statistics of our measurements allowed us to obtain, at each temperature, the relative spin density (in momentum space) of Ni in the (100) plane. These distributions are presented on the same scale in figure 5. A curve extracted from each spectrum in the [110] direction is also drawn in figure 6 in order to make the statistical error appreciable. The two-dimensional spin density of Ni exhibits a rather important negative part around $p = 0$ which is absent in the experimental spin-polarized Compton profiles of Ni (Mills 1987). There is, however, no contradiction between the two measurements; as in the case of Fe (Genoud *et al* 1988, Genoud and Singh 1989), this is attributed to the important overlap of the positron wave function with that of the s and p electrons whose polarization is predicted to be negative by standard band-structure calulations. The manifestation of this negative polarization of s and p electrons in the experimental spin-polarized Compton profiles is the central dip exhibited by the curves.

When the temperature increases to T_{Curie}, the volume of the distribution diminishes without any change in the structures. This behaviour principally reflects the corresponding reduction of the saturation magnetization of the sample when approaching T_{Curie}. To illustrate this point we have calculated the magnetization curve of a system of kinetic moment $J = \frac{1}{2}$ under a magnetic field of 4 T, using the Weiss equation:

$$M_s/M_0 = \tanh[(M_s/M_0 + H/NM_0)/(T/T_{\text{Curie}})] \tag{7}$$

where M_s is the saturation magnetization, M_0 the saturation magnetization at $T = 0$, H the external magnetic field and N the molecular field constant for Ni (see for example Bozorth 1951). A similar curve calculated for a field of 1.8 T describes relatively well

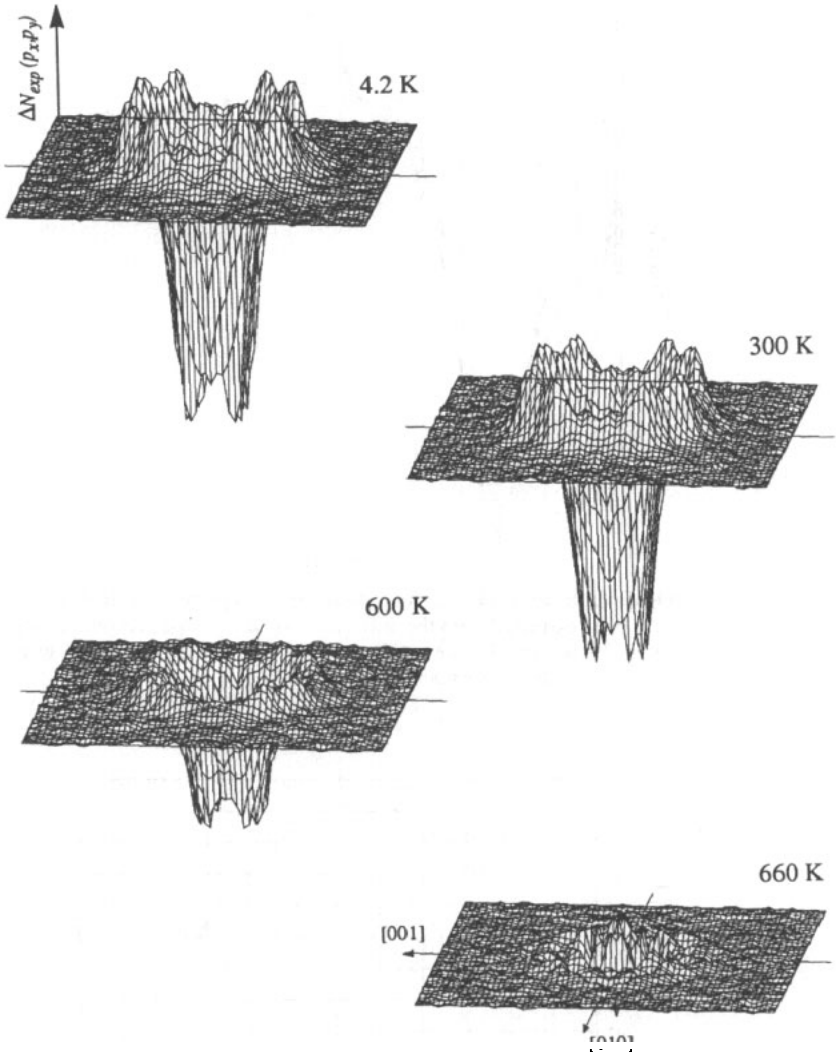

Figure 5. 2D ACAR distributions of Ni in the (100) plane at different temperatures: relative spin density $\Delta N(p_x, p_y)$. The measurements have been carried out at 4.2, 300, 600 and 660 K. The scale is common to each graphic. The spectra cover a region extending to ±20 mrad in each direction and the Curie temperature is 627 K.

the corresponding measurements made on Ni by Weiss and Forrer 1964). The volume of each relative spin density distribution has been compared with that of the relative spin density at 4.2 K. The four corresponding values are reported in figure 7 together with the above calculation. The points which correspond to the measurements performed below T_{Curie} follow the magnetization curve relatively well. Assuming a positron distribution independent of temperature, part of the remaining discrepancies can be understood in terms of a temperature-dependent depolarization of the positrons during the thermalization process. This has been observed in Fe and Seeger *et al* (1987) who have

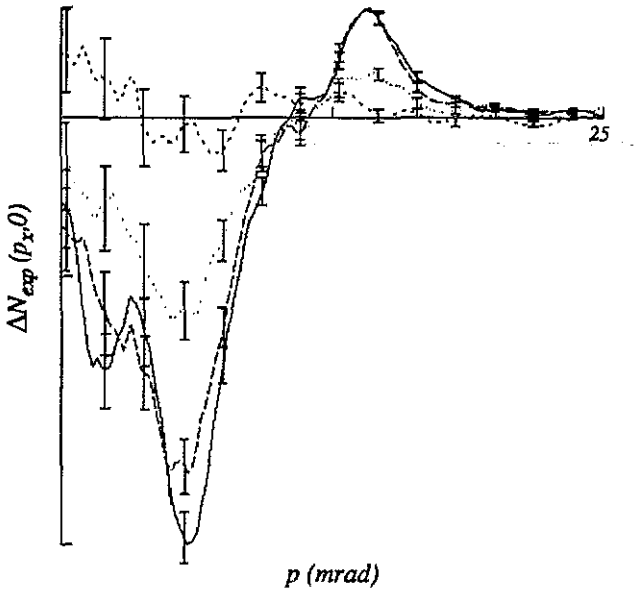

Figure 6. Relative spin density of Ni in the (100) plane at different temperatures. The lines have been extracted from the distributions in the [110] direction. Full curve: 4.2 K, broken curve: 300 K, dotted curve: 600 K, frequently broken curve: 660 K. The error bars represent each statistically independent point.

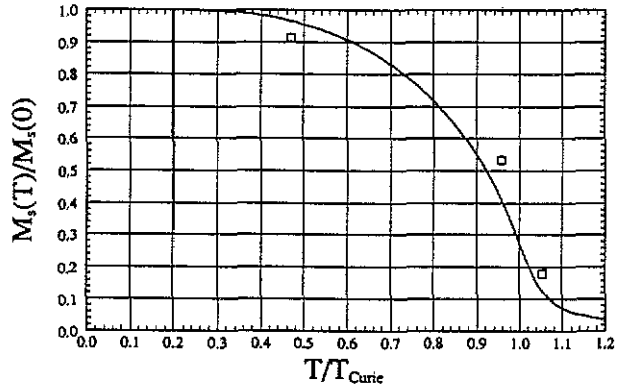

Figure 7. Saturation magnetization of Ni as a function of temperature calculated for $J = \frac{1}{2}$ and for a magnetic field of 4 T in the Weiss theory (full curve). The squares represent the volume of the relative spin density distributions compared with that of the measurement at 4.2 K (see text).

measured the polarization P_p of the annihilating positrons as a function of temperature. These authors have reported both increasing and decreasing P_p with temperature, according to the magnitude of the applied magnetic field. The relative differences amount to 4%. No such measurement has, however, been made in Ni. We have also to keep in mind the fact that we are only dealing with relative distributions; the term

$\rho^{2\gamma}_{maj}/\rho^{2\gamma}_{min}$ of equation (5) indicates that the spectra shown in figure 5 do not exactly represent $\rho^{2\gamma}_{min}(p_z, p_y) - \rho^{2\gamma}_{maj}(p_x, p_y)$. The contribution of the minority electrons is weighted by a factor that is equal to 1.0357 according to IPM calculations (Singh *et al* 1986). Electron–positron correlation effects should not change this value drastically (Genoud 1990). The effect of temperature (thermal motion of the positron) could also affect the distributions. We estimate that the experimental resolution at 660 K is more than twice that at 4.2 K. But this effect should not be important when compared with that of the smoothing procedure applied to the relative spin density distributions.

Above T_{Curie} the volume of the relative spin density distribution remains appreciable since we are not in the paramagnetic state. However, the spectrum differs qualitatively from that observed at lower temperatures in that the positive polarization at high p ($p \geq 10$ mrad) attributed to d electrons almost disappears; we also note a region of positive polarization around $p = 0$ that is totally absent at 600 K and below. We are, however, unable to explain this observation (mainly because of the lack of comparison points).

5. Conclusion

The 2D ACAR data measured on a single crystal of Ni in the (100) plane at 4.2, 300, 600 and 660 K have been analysed both in k space (using the LCW theorem) and in p space. No appreciable difference has been observed between the total distributions obtained below the Curie temperature. Then a straightforward conclusion would be that the exchange splitting of Ni is essentially independent of temperature. This is, however, moderated by the LMTO calculations we have performed in order to simulate a decrease of Δ with increasing temperature. The analysis of the calculated 2D ACARs does not exclude a variation of Δ of about 28% between 4.2 and 600 K. Anyway our conclusions exclude the important variation of Δ proposed by Hopster *et al* (1983) and by Gerhard (1983) on the basis of angle-resolved photoemission spectroscopy. However, they are consistent with the spin-polarized electron-energy-loss spectroscopy results of Kirschner and Langenbach (1988) who predict a temperature-independent exchange splitting in Ni up to the Curie temperature.

The variation of the volume of the spin density data can be crudely related to the reduction of the magnetization of Ni when the temperature increases. It is, however, difficult to interpret the structures observed above the Curie temperature. To get a clearer picture of the situation we think that more investigations have to be performed near the Curie temperature in ferromagnetic materials. Moreover, the measurement of data for purely paramagnetic metals at high temperature is highly desirable. The present work shows the potential and the importance of positron annihilation technique (and especially 2D ACAR) in studying magnetic materials at low as well as at high temperatures.

Acknowledgments

It is a pleasure to thank T Jarlborg, A K Singh and L Hoffmann for stimulating discussions and for their remarks concerning the drafting of this manuscript. This work was supported by the Fonds National Suisse de la Recherche Scientifique.

References

Badwell M O and Paulus T J 1979 *Proc. Int. Conf. Positron Annihilation (ICPA5)* ed R R Hasiguti and K Fujiwara (Sendai: Japan Inst. Met.) p 375

Berko S 1977 *Compton Scattering* ed B Williams (London: McGraw-Hill) p 273

Berko S and Mills A P 1971 *J. Physique Coll.* **23** C1 287

Berko S and Zuckermann J 1964 *Phys. Rev. Lett.* **13** 339

Bisson P E, Descouts P, Dupanloup A, Manuel A A, Perreard E, Peter M and Sachot R 1982 *Helv. Phys. Acta* **55** 110

Blank R, Schimmele L and Seeger A 1988 Proc. ICPA8 *Positron Annihilation* ed L Dorikens *et al* (Singapore: World-Scientific) p 278

Bozorth R M 1951 *Ferromagnetism* (New York: van Nostrand) p 717

Genoud P 1990 *PhD Thesis* No 2442 University of Geneva

Genoud P and Singh A K 1989 *J. Phys.: Condens. Matter* **1** 5363

Genoud P, Singh A K, Manuel A A, Jarlborg T, Walker E, Peter M and Weller M 1988 *J. Phys. F: Met. Phys.* **18** 1933

Gerhard U 1983 *Helv. Phys. Acta* **56** 105

Hanna S S and Preston R S 1958 *Phys. Rev.* **109** 716

Hoffmann K R, Berko S and Beaudry B J 1982 Proc. ICPA6 *Positron Annihilation* ed P G Coleman *et al* (Amsterdam: North-Holland) p 325

Hopster H, Raue R, Güntherodt G, Kisker E, Clauberg R and Campagna M 1983 *Phys. Rev. Lett.* **51** 829

Jarlborg T, Manuel A A, Mathys Y, Peter M, Singh A K and Walker E 1986 *J. Magn. Magn. Mater.* **54** 1023

Jarlborg T and Singh A K 1987 *Phys. Rev.* B **36** 4660

Kirschner D and Langenbach E 1988 *Solid State Commun.* **66** 761

Kontrym-Sznadj Stachowiak H, Wierzchowski W, Petersen K, Thrane N and Trumpy G 1975 *Appl. Phys.* **8** 151

Lock D G, Crisp V H C and West R N 1973 *J. Phys. F: Met. Phys.* **3** 561

Mijnarends P E 1979 *Positrons in Solids* ed P Hautojärvi (Berlin: Springer) p 25

Mills D M 1987 *Phys. Rev.* B **36** 6178

Page L A 1959 *Rev. Mod. Phys.* **31** 759

Rabou L P L M 1983 *PhD Thesis* University of Amsterdam

Seeger A, Mayer J and Banhart F 1987 *Phys. Status Solidi* a **102** 91

Singh A K and Jarlborg T 1985 *J. Phys. F: Met. Phys.* **15** 727

Singh A K, Manuel A A, Jarlborg T, Mathys Y, Walker E and Peter M 1986 *Helv. Phys. Acta* **59** 410

Sormann H 1988 *Proc. Positron Annihilation Int. Conf. (ICPA8)* ed L Dorikens *et al* (Singapore: World-Scientific) p 5272

Weiss P and Forrer R 1964 *C. R. Acad. Sci., Paris* **178** 1670

Yousuf M, Sahu P C and Govinda Rajan K 1986 *Phil. Mag.* B **54** 241